Technical Report for Incorporated Engineer - Structural Mechanics of a Broken Rail & Rail Risk Score of Rail for the West Coast Mainline

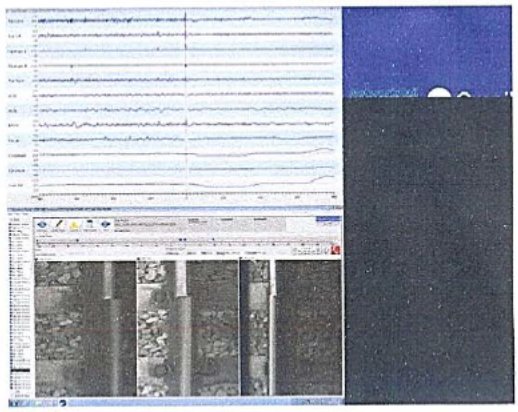

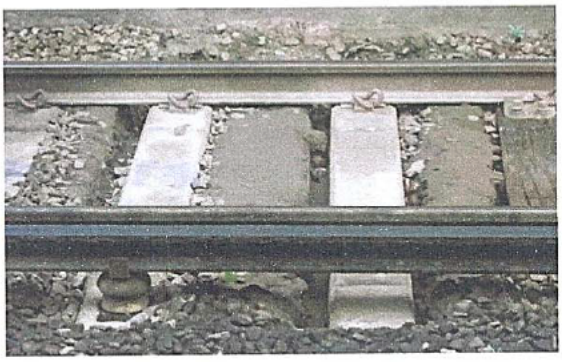

[redacted]

Table of Contents

1.0 Table of Figures

2.0 Definitions

- **Ballast –** Stone pieces (usually granite) sized 62mm or smaller and graded to NR/L2/TRK/8100 Railway Ballast and Stoneblower aggregate (Evans, et al., 2009). Ballast distributes loading through to the formation and subgrade layers and provides rapid dispersal of water.
- **Broken Rail –** See rail break.
- **Bullhead rail –** Historically the rail section used across the UK network, bullhead rail was invented in 1835 by Joseph Locke (The Permanent Way Institution, 2014) both head and foot of the rail are the same dimension; the original intention was to turn the rail over once the top was worn. In practice this was not possible as the underside would become worn under traffic. Later iterations of bullhead rail had a larger head and smaller foot. Bullhead rail will not stand unaided and is supported in cast iron chairs.
- **Cant –** Also known as Superelevation, the elevation of one rail above the other to lean a vehicle into a curve aiding steering.
- **Cant deficiency –** if the equilibrium cant is not fully applied the remaining amount is described as cant deficiency
- **Continuously welded rail –** Rails welded together to form a continuous running surface without joints.
- **Dip angle –** A dip angle is a local reduction in rail level measured at the centre point of a one metre straight edge centred on the height reduction in the rail measured in milliradians. A 4 milliradian (mrad) dip at the 500mm point of the straight edge is equivalent to a 1mm reduction in height.
- **Dynamic Loading –** The load exerted by the vehicle when travelling at speed and including other relevant details from GM/TT0088 Permissible Track Forces For Railway Vehicles (British Railways Board, 1993)
- **Equilibrium Cant –** The cant required for a given curvature and linespeed to make a vehicle traverse a curve without lateral forces enacting upon it.
- **Fishplate –** A plate of cast iron used to connect two rails together.
- **Flat Bottom Rail –** Trialled from the 1940's Flat bottom rail has a flat foot so will stand unaided and is considerably stronger in bending than bullhead. In 1948 British Railways adopted 109lb (pounds per yard) flat bottom for all renewals on mainlines. In 1968 BS113a (later renamed CEN56 [kilograms per metre]) was adopted for all renewals. This rail section is still used today. In addition CEN60 rail is now used on main line routes.
- **Formation –** prepared materials between the ballast and subgrade, used to provide additional strengthening, or to avoid contamination or deterioration of the ballast from the subgrade materials.
- **Four foot –** the area between the two running rails of a railway line.
- **Gauge Face –** The face of the rail in the four foot, which interacts with the flange of the wheel in certain scenarios.
- **Hanging –** See voiding
- **Jointed Track –** Track forms with rails in lengths (nominally 60 ft) connected together with fishplates and bolts.
- **Rail –** The longitudinal beams which support the train and provide directional guidance.

- **Rail Break –** A rail break is defined as a crack through the steel of the rail separating the material into two separate pieces.
- **Rail Pads –** Concrete sleepers are fitted with a rail pad between the rail and the sleeper to reduce attrition between the two and electrically insulate. Pads are either of a 5mm or 10mm thickness and made from rubber or rubber bonded cork. Rail pads can also be changed to allow for wear in other components for example a 5mm pad can be replaced with a 7.5mm maintenance pad.
- **Route Availability (RA) –** The system Network Rail uses to grade a routes ability to withstand a load from RA1 (weakest) to RA10 (strongest). Rolling stock is graded with the same system, the item of rolling stock must have a RA number lower than or equal to than the route it is travelling on.
- **Running Table –** Term used to describe the continuous running surface of the rail.
- **Sleepers –** The lateral restraints to hold the two rails at the correct interval and transfer load from the rail downward into the ballast. For the purpose of this report all sleepers are assumed concrete monobloc, other types of sleeper make up less than 1% of the area considered by the report. (Network Rail, 2017)
- **Static Loading –**The load exerted by the weight of the vehicle when stationary.
- **Sub-grade –** the underlying ground on which the railway is sited, could be of natural formation 'at grade' or a prepared embankment or cutting. Could be many geological substances.
- **Trace or Track Trace –** The trace is a plot of all the data provided by the track recording vehicle in direction of travel.
- **Track Category –** Network Rail's track infrastructure is all assigned a track category, this is as defined in NR/L2/TRK/2102. The track category is a product of the line speed and tonnage of a line. Category 1A is the most used track with highest line speeds down to Category 5 the lowest used. Network Rail uses the track category to determine the appropriate whole life asset management strategy for a given line.
- **Track system –** The collective term used for Rail, Sleepers, Ballast, Formation and Sub-grade as defined above.
- **Track Top –** Measured on a 35m wavelength or 70m wavelength by the Network Rail Track recording vehicles or from manual recording with a trolley. Top is a measure of track quality in the vertical plain. The trace plot for top left (left rail) and top right (right rail) shows the difference in level between highest point and lowest point of the rail over the wavelength stated (NR/GN/TRK/7001/TWI3T046/Video9 Track Recording Vehicle Vertical Level or Top Fault, 2013).
- **Voiding –** Term used to describe vertical deflection of the sleepers and rail under traffic. Voiding is caused when insufficient consolidation of the ballast layer has been achieved, or when consolidation has deteriorated under loading. A void will build up beneath the sleeper and allow the track to move vertically.
- **Wetbed –** A wetbed is an area of formation failure which has been significant enough to liquidise the ballast which has also mixed with contaminants from beneath (mud silts or clay) during a wet period. A wetbed can also then set hard during a dry period.

2.2 Abbreviations

- BS — British Standard – In the context of this report used in rail grading I.E BS113a
- CEN — Comité Européen de Normalisation – In the context of this report used in rail grading I.E CEN56
- CWR — Continuously Welded Rail
- KN — Kilonewton
- KNM — Kilonewton Metres
- LNW — London North Western (Network Rail Route Business)
- m — Metre
- mm — Milimetre
- MC — Bending Moment
- mrad — Milliradians
- MN/m^2 — Mega Newton's per metre Squared
- N — Newton
- ORR — Office of Rail and Road, Formerly Office of Rail Regulation pre April 2015
- PWI — Permanent Way Institution
- Ra — Reaction A
- RA — Route Availability
- Rb — Reaction B
- RAIB — Rail Accident Investigation Branch
- RCF — Rolling Contact Fatigue
- RSSB — Rail Safety and Standards Board
- t — Tonne (Metric)
- V — Shear Force
- WCML — West Coast Main Line
- Σ — Summation of

3.0 Executive Summary

Throughout the report below I have calculated load that rail in service on the West Coast Main Line (WCML) has imposed upon it in normal service as well as studying industry accepted research to identify key trends and risks. Key findings of the report are that highest loadings are created at high speed at positions of either a sudden change in the running table i.e at a dip angle or where the support conditions are variable. I have used the report to create 'WCML Broken Rail Risk Tool'. I intend to present the tool to Network Rail's London North Western (LNW) Route Buisness for trial use. Example reports from the tool are available in Appendix B of this document.

4.0 Introduction

It is the purpose of this report to demonstrate I have gained sufficient knowledge and experience, through my career as a track engineer, to address the difference between my base qualification of HNC with distinction and the requirement of Bachelor's Degree for Incorporated Engineer.

4.1 Background

A broken rail is a key risk to the safe passage of trains on the infrastructure, in most cases a rail breaks through cleanly leaving a minimal gap in the running table. However in rare cases such as the Hatfield derailment October 2000 (Office of Rail Regulation, 2006) rail can break in an uncontrolled way leaving a significant gap in the running table. This caused the derailment of rail vehicles travelling at 115mph and as a result four people lost their lives and seventy were injured (Office of Rail Regulation, 2006). This report found many causal factors as to why the rail broke in such a manner, however key outcomes were change to Ultrasonic testing including the introduction of the Ultrasonic test train, Network Rail's decision to move maintenance of the railway back in house to increase their level of control, increased government investment in the railways, enhancement to rail grinding regimes and better information on all rail accidents and incidents through the formation of The Rail Accident Investigation Branch (RAIB) (Office of Rail Regulation, 2006). These improvements have greatly reduced the number of broken rails over time.

Figure 1 Typical photo of a broken rail demonstrating the 'clean' nature of the break

5.0 Problem Statement

As stated in section 4.0, since 2000, broken rail numbers have decreased and are now at a historic low. A paper presented to Network Rail Track Leadership Group (Whitney, 2015) finds the majority of broken rails now occur in a sudden and less predictable way. The paper details that these rail breaks are generally associated with other factors which affect the loading of the rail, for example a change in track stiffness. There is currently no way to calculate site risk for its potential to have a broken rail, thus maintenance and renewal strategies currently applied from the national level may be overly conservative, or overly generous depending on site specifics for the management of the rail.

6.0 Aim

In this report I intend to demonstrate the structural properties of UK standard rail profiles. I will go on to develop this by demonstrating how these properties change under operating conditions, to either increase the rail's loading or weaken the rail. I will use the calculations I have undertaken to assign a weighting factor to each type of change in loading and then create a tool to calculate rail break potential for the West Coast Main Line.

7.0 Scope, Assumptions and Exclusions

For the purpose of this report I will limit the scope geographically to the West Coast Main Line (WCML) between London Euston and Rugby. As the area of Network Rail's London North Western (LNW) Route Business with the highest tonnage and maximum line speed this has the highest potential for failure and the biggest impact to our customers should such a failure occur. I have used the current highest axle load of 25.4 tonnes, based on Network Rail's route availability RA 10 for the route (Network Rail, 2017) for all calculations except where otherwise stated.

Calculations of potential for breaks at rail joints are excluded from this report due to the continuously welded rail nature of the majority of the area stated above, in which jointed track makes up less than one percent (Network Rail, 2017).

1 metric tonne force is converted to 9.80665 Kilonewtons (KN) throughout. Numerical values are rounded to 3 decimal places unless otherwise stated, rounding's are applied to the final answer of equations. All lengths are shown in metres unless stated otherwise. Drawings are not to scale unless specified otherwise. The scope of this report is limited to failures manifesting in the rail; however, to understand the modes in which this failure happens, it is necessary to consider factors in the track system as a whole. Slab track, Switches and Crossings (S&C), directly fixed structures and structures with longitudinal timbers are excluded.

7.1 Failure modes of rails leading to rail breaks

It is commonly accepted in structural mechanics that short beams, as a rail can be considered, fail in shear and from my own experience and research (Network Rail LNW Route, 2016) this holds true for almost all rail breaks. I will go on to look at the forces involved and why mathematically this is the case in section 9 of this report. However it is normal for another factor or factors to be involved at the point of the break creating a weakness in the rail.

Tensile failure emanating from a corrosion pit in the foot of the rail, has been, in recent years, the most common cause of failure in rail. All steel rails have some corrosion in normal service; corrosion resistant rails are only used in extreme scenarios such as tunnels and coastal areas. Corrosion related breaks usually manifest from a corrosion pit in the foot of the rail. These are undetectable ultrasonically, however it is theorised that they exist in rails all over the network and are benign until another factor, for example a dip angle, increases the loading, causing the rail to abruptly fail.

Figure 2 Broken Rail showing a corrosion pit

Fatigue manifests itself in rails as rolling contact fatigue (RCF) eventually causing gauge corner cracking and the rail to break. This failure mode led to the broken rail and derailment at Hatfield in 2000 (Office of Rail Regulation, 2006). Given this history it has a serious consequence if left unmanaged. However as discussed in earlier sections, improvements in grinding and ultrasonic inspection have meant that rail breaks from this mechanism have become rare. This is as would be expected given its slow propagation.

Manufacturing defects in the rail itself can cause a broken rail. This is particularly prevalent in rails rolled prior to 1976. Post 1976 the manufacturing process for rail changed from the previous ingot method to a continuous casting process (concast) method. The change has dual benefits of reducing problem elements from the steel and using less energy in casting. These types of failures manifest themselves as a tache ovale (The Permanent Way Institution, 2014) and are generally detectable through ultrasonic methods.

At a rail joint or weld, although excluded from this report, fishplate joints and welds can be a further position at which a rail can break. Fishplates tend to break when the joints are significantly dipped causing addition loading. Welds are likely to fail if the casting process was not fully successful.

Wear is a final method in which rail can fail. Rail wears either from the top with its depth reducing over a long period or on curved track the wear will occur in the gauge corner, this is known as sidewear. As with RCF this is a slow and predictable failure mode and well embedded inspection maintenance and renewal practice means that failure from this mode is now also rare.

8.0 Research

To improve my understanding of the engineering concepts discussed in this paper, I read the following publications as background reading.

- Understanding Track Engineering (The Permanent Way Institution, 2014)
- A Guide to Track Stiffness (Powrie & Pen, 2016)

- Train Derailment at Hatfield: A Final Report by the Independent Investigation Board (Office of Rail Regulation, 2006)
- TEF 3064 Hazard Report for Track Assets – WCML reports on Broken Rails (Network Rail LNW Route, 2016)
- GM/TT0088 Permissible Track Forces For Railway Vehicles (British Railways Board, 1993) and the associated guidance document GMRC2513 Issue 1 Commentary on Permissible Track Forces for Railway Vehicles (Boocock & Mitchell, 1995)
- RAIB Report: Class investigation into rail breaks on the East Coast Main Line (RAIB, 2017)

Where information has been cited from appropriate literature, standards or systems I have cited the source in section 12 of this report.

9.0 Analysis

9.1 Calculations for Ideal Operating Scenario

In order to accurately understand why rails break and what factors will make this more or less likely I will calculate the forces acting upon the rail.

Rail is a continuously supported beam on an elastic foundation. To simplify calculations in the subsequent section I will treat the rail as a beam between two sleepers, acting as its support. This will also give worst case values. I will start by assuming that the sleepers are sufficiently supported by the ballast and subgrade to resist all forces acting upon them, meaning the beam is in equilibrium. The axle load has been given in section 7.0 above; from this I have taken the loading on each rail to be 12.7t or 124.544KN. I have used 0.65m as the beam length, this is current standard centre to centre sleeper spacing for Track Category 1A track (Whitney, et al., 2016). My calculations are shown in the figures below. Supporting calculations can be found in Appendix A. The rail is referred to as beam AB throughout.

9.1.1 Calculations of Reactions at supporting sleepers

The sum of all vertical forces (ΣVF) is 0 in this example as beam AB is in equilibrium – I can therefore calculate the reactions and moments at Ra & Rb which are both 62.272KN.

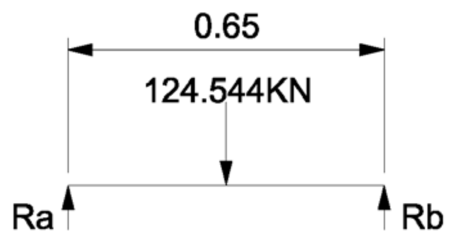

Figure 3 Force and reactions in Beam AB wheel loading at mid-span

9.1.2 Free body diagram

The free body diagram for the beam is as shown below

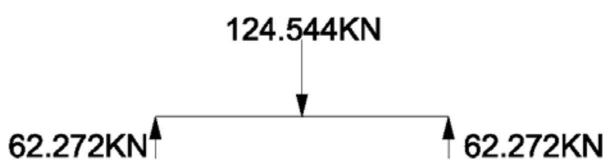

Figure 4 Free Body Diagram Beam AB wheel loading at mid-span

9.1.3 Calculation of Bending Moment at Mid-span

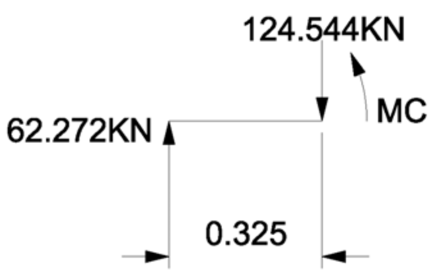

Figure 5 Showing Beam AB cut at the mid-span and moment MC wheel loading at mid-span

With the value of the reactions at Ra and Rb now known it is possible for me to calculate the Bending moment at point C at mid-span as shown in the above figure. I can now form an equation to solve for MC – Which is 20.238KNM.

9.1.4 Bending Moment Diagram

The Bending Moment diagram for the beam is shown below

Figure 6 Bending Moment Diagram for Beam AB wheel loading at mid-span

9.1.5 Shear Force

I can calculate the shear force at any point in the beam by working across the beam and calculating the summation of forces acting on the beam moving left to right. The maximum shear force in the beam is 62.272KN

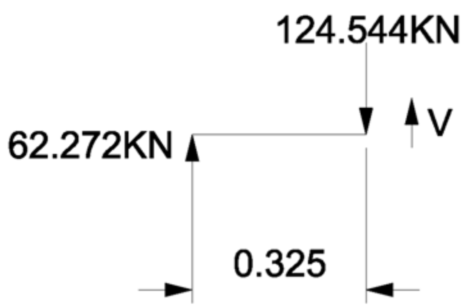

Figure 7 Shear Force V at mid-span of beam AB wheel loading at mid-span

9.1.6 Shear Force Diagram

The Shear Force diagram for the beam is shown below

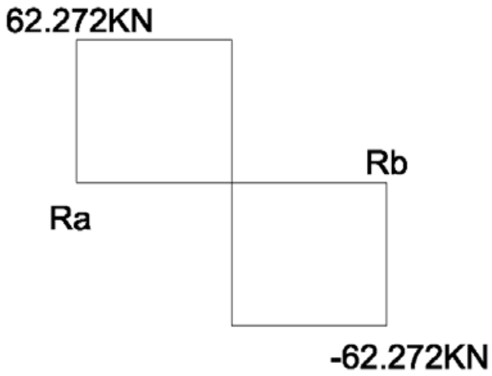

Figure 8 Shear Force diagram Beam AB wheel loading at mid-span

9.1.7 Change as the load moves across beam AB

The calculations in the above sections show the load at mid-span. Theoretically the shear force will increase and the bending moment decrease as the load from the wheel moves to the extremities of the beam. In the calculations below I have shown the load acting at 0.143m from Reaction A. This distance represents the width from the centre to edge of a G44 concrete sleeper (Downes, et al., 2016) the standard sleeper for this route since 2000. Following the previous process Ra = 97.144KN and Rb = 27.400KN

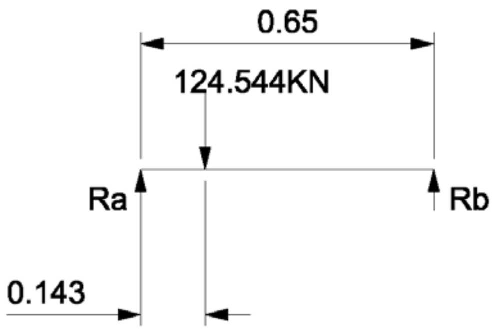

Figure 9 Force and reactions in Beam AB wheel loading at edge of sleeper

9.1.8 Free body diagram

The free body diagram for the beam is as shown below

Figure 10 Free Body Diagram Beam AB wheel loading at edge of sleeper

9.1.9 Calculation of bending moment at sleeper edge

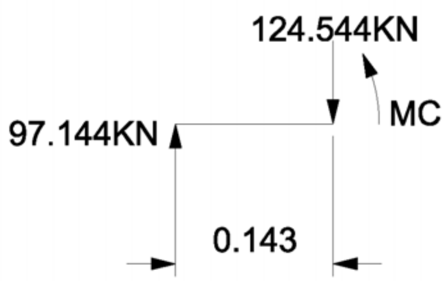

Figure 11 Showing Beam AB cut at the mid-span and moment MC wheel loading at edge of sleeper

The maximum bending moment is 13.891KN

9.1.10 Bending Moment Diagram

The Bending Moment diagram for the beam is shown below

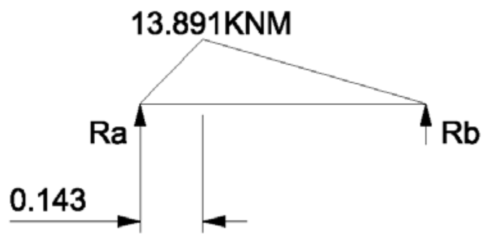

Figure 12 Bending Moment Diagram for Beam AB wheel loading at edge of sleeper

9.1.11 Shear Force

The maximum shear force in the beam is 97.144KN.

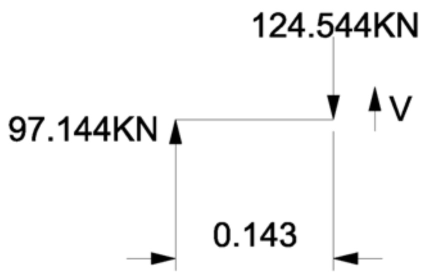

Figure 13 Shear Force V at mid-span of beam AB wheel loading at edge of sleeper

9.1.12 Shear Force Diagram

The Shear Force diagram for the beam is shown below

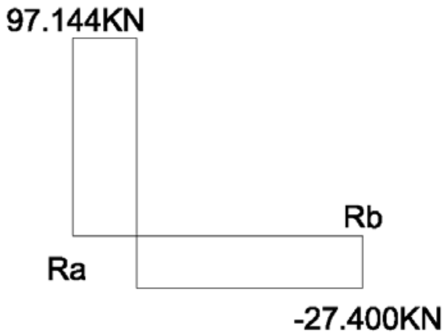

Figure 14 Shear Force diagram Beam AB wheel loading at edge of sleeper

9.1.13 Findings of Section 9.1

Throughout the section above I have shown the shear stress to be the highest force acting in the beam. This validates common structural mechanics thinking that short beams (such as AB) are more likely to fail in shear. My second finding is that the shear force increases as the wheel loading moves towards the edge of the beam, this validates research I have undertaken on actual broken rails from WCML like those shown in figure 13 below. (Network Rail LNW Route, 2016)

Figure 15 Photos from TEF3064 reports of actual broken rails from Kilsby Tunnel and Bourne End on the West Coast Main Line respectively

9.2 Dynamic Loading

In this section I intend to expand upon the previous findings to show how the dynamic load on the rail increases. I intend to look at two cases a Class 390 Pendolino Vehicle travelling at 125mph as a worst case speed scenario, and a laden freight vehicle travelling at 75mph as a worst case mass scenario. To do this I have used the formula set out in Railway Group Standard GM/TT0088 (British Railways Board, 1993). This standard, though from 1993 is still current and has been taken from the RSSB Railway Group Standards so is still applicable to the whole of the rail industry. Clause 6.2 of the standard is shown below giving the base formula I will use.

British Railways Board Uncontrolled When Printed **Group Standard**

Permissible Track Forces for Railway Vehicles

GM/TT0088
Issue: 1
Revision: A
Date: OCT 1993
Page 7 of 11

6 Vertical Dynamic Forces

6.1 Vehicles shall be able to run over the normal range of vertical track irregularities at normal operating speeds without generating excessive vertical loads and stresses in the rails and track.

6.2 Except as in Clause 6.3, a vehicle shall be able to negotiate a vertical ramp discontinuity in rail top profile, equivalent to a dipped rail joint on straight track, at its maximum design operating speed without exceeding a total (static plus dynamic) P2 force per wheel of 322 kN.

The P2 force shall be calculated using the following formula:

$$P_2 = Q + (A_z . V_m . M . C . K)$$

where

$$M = \left[\frac{M_v}{M_v + M_z}\right]^{0.5}$$

$$C = 1 - \left[\frac{\pi . C_z}{4[K_z(M_v + M_z)]^{0.5}}\right]$$

$$K = (K_z . M_v)^{0.5}$$

Q = maximum static wheel load (N)

V_m = maximum normal operating speed (m/s)

M_v = effective vertical unsprung mass per wheel (kg)

A_z = 0.020 rad
(total angle of vertical ramp discontinuity)

M_z = 245 kg
(effective vertical rail mass per wheel)

$C_z = 55.4 \times 10^3$ Ns/m
(effective vertical rail damping rate per wheel)

$K_z = 62.0 \times 10^6$ N/m
(effective vertical rail stiffness per wheel)

Figure 16 Extract of page 7 GM/TT0088 (British Railways Board, 1993)

9.2.1 Passenger vehicle case – Class 390 travelling at 125mph (55.88m/s).

From the formula above I will substitute the following values

Q – 73549.875N – Based on 7.5t per wheel from the class 390 Axle loading of 15t (4rail.net, 2004-2010)

Vm – 55.88 m/s

Mv 1000 kg (normal unsprung mass for high speed trains with distributed power) (Ventry, et al., 2002)

From this I have determined the dynamic load of the vehicle is equivalent to 283742.669N or 283.742KN. This is an increase of 159.179 KN on the maximum static loading used in the previous calculations and 259% of the original Static vehicle load.

9.2.2 Freight Vehicle Case – 4 Axle Steel Wagon travelling at 75mph (33.53m/s)

I will repeat the calculation for a laden fright vehicle as this represents the vehicle with the highest mass. This is equivalent laden weight of 102t based on a 4 axle vehicle (RSSB, 2015) (e.g. Steel trains). The values I will be using are below

Q – 124544N

Vm – 33.53m/s

Mv – 950kg (normal unsprung mass for 25.5t axle load freight vehicles non-powered) (Ventry, et al., 2002)

From this I have determined the dynamic load of the vehicle is equivalent to 246489.376N or 246.489KN. This is an increase of 121.945 KN on the vehicle static loading used in the previous calculations and 197% of the original static vehicle load.

9.2.3 Findings from Section 9.2

In the above section I have used formulas provided in Railway Group Standards supplemented with additional research I have conducted into vehicles using the route to model the effect dynamic loading have on the force exerted at rail level. The highest force is as exerted by a high speed passenger train. Despite the initial significantly lower static load of this vehicle the higher unsprung mass and faster speed make it the most damaging case.

9.3 The dynamic effect of dip angles

The Research conducted on broken rails on the WCML as a part of the paper *'West Coast Main Line the Day Job and Beyond'* presented to the PWI in May 2017 (Green, et al., 2017) showed an unbroken correlation between broken rails and the presence of dip angles. The formula above includes a factor to represent a dipped joint of 20mrad value Az. As stated in section 7.0 above the geographical scope of this report is limited to continuously welded rail however the research paper shows me that dip angles are present within this scope. I will use the formula above taken for the class 390 train at linespeed and use it to model a series of dip angles at different values to model the increase in load this forms in the rail.

9.3.1 30mrad dip angle, Network Rails Maintenance Intervention Limit

Network Rail's Standard NR/L2/TRK/001 Inspection and Maintenance of Permanent way issue 11 (Whitney, et al., 2017) shows a dip angle of 30mrad on track with a linespeed of 90mph or greater as a repair within 13 weeks fault. I will repeat the formula from section 10.2.1 changing the dip angle value to 30mrad

In this scenario the load has increased to 389.819KN an increase of 106kN on the dynamic loading for a 20mrad dip angle.

9.3.2 20mrad dip angle, LNW Letter of Instruction Intervention Limit

Following first identification of an increasing trend of broken rails associated to dip angles LNW Route Business issued Letter of Instruction 15722 in December 2013 (Webb, 2013) which amended the value of 30mrad given in Network Rail Standards (Whitney, et al., 2017) to 20mrad. The calculation for this value is as the previously worked example I provided in 10.2.1. The dynamic force exerted is 283.723KN.

9.3.3 10mrad dip angle, minimum identified by current track recording methods

The current track recording fleet report dip angles from 10mrad. I will again repeat the calculation with the smaller dip angle measurement.

In this scenario the load has decreased to 178.626KN a decrease of 105kN on the dynamic loading for a 20mrad dip angle.

9.3.4 4mrad dip angle 1mm reduction in height

Finally I will repeat the process for a 4mrad dip angle which is, in theory, is a 1mm reduction in height over a 1m straight edge. Due to imperfections in the rail from manufacturing it is unlikely that rail would ever be completely flat. So, in practice, this scenario would represent the dynamic loading on the rail without a dip angle fault of any sort. Effectively a 4mrad dip angle would not be measurable in the field.

In this scenario the load has decreased to 115.588KN a decrease of 168kN on the dynamic loading for a 20mrad dip angle.

9.3.5 Findings of section 9.3

The section shows that reduction of the mrad intervention point for dip angles has a significant impact on reducing the load being dynamically transmitted to the rail. This supports the LNW local instruction (Webb, 2013) and would justify the industry to research the merits of looking to further reduce the intervention point.

9.4 Dynamic loading calculations

From Section 9.1 above the highest loading is in shear and when the loading is applied at sleeper edge I will repeat the calculations for a series of dynamic loadings with dip angles to give real values of loading in rail.

I have excluded 30mrad dip angles as these have been removed from LNW following the local instruction.

9.4.2 Calculation of forces at sleeper edge for Class 390 dynamic loadings

9.4.3 20mrad dip angle

Repeating the calculations from previous sections, I have calculated the following values.
Ra=221.304KN, Rb=62.419KN.

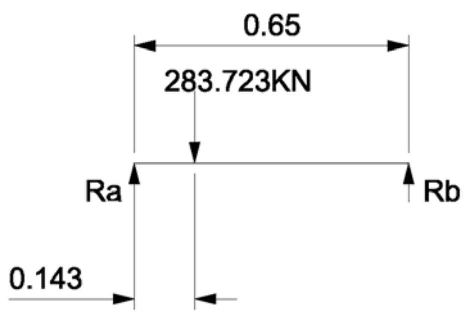

Figure 17 Force and reactions in Beam AB wheel loading at edge of sleeper

9.4.4 Free body diagram

The free body diagram for the beam is as shown below

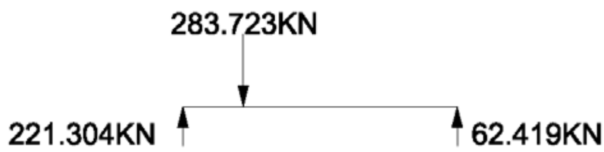

Figure 18 Free Body Diagram Beam AB wheel loading at edge of sleeper 20mrad dynamic loading

9.4.5 Bending moment calculations

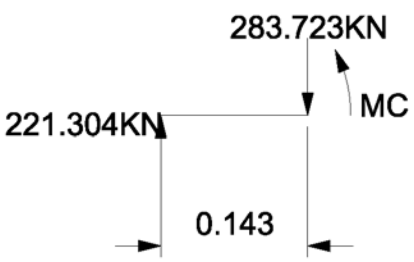

Figure 19 Showing Beam AB cut at the mid-span and moment MC wheel loading at edge of sleeper 20 mrad dip angle

The Maximum bending moment in this scenario is 31.646KNM.

9.4.6 Bending Moment Diagram

The bending moment diagram for the beam is shown below

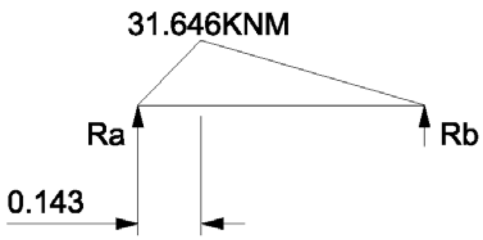

Figure 20 Bending Moment Diagram for Beam AB wheel loading at edge of sleeper 20mrad dip angle

9.4.7 Shear Force

The maximum shear force in this scenario is 221.304KN

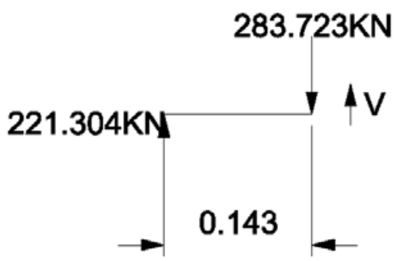

Figure 21 Shear Force V at mid-span of beam AB wheel loading at edge of sleeper 20mrad dip angle

9.4.8 Shear Force Diagram

The shear force diagram for the beam is shown below

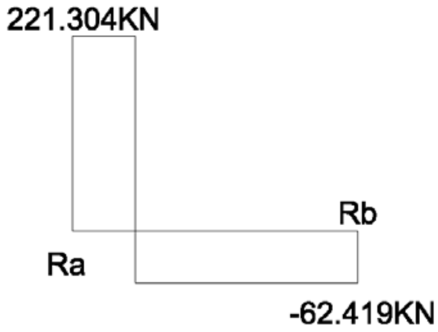

Figure 22 Shear Force diagram Beam AB wheel loading at edge of sleeper 20mrad dip angle

9.4.9 Dynamic loadings for 10mrad dip angle

I have completed similar calculations for 10mrad dip angle, this gives a Ra of 139.298kN, Rb of 39.298kN MC of 19.924kNm. The maximum shear force in the rail is 139.328kN.

9.4.10 Fatigue at dip angles

It is also an important consideration that rail undergoes a repeated loading and unloading cycle. Fatigue is therefore a key consideration in all types of rail failure. Dip angles have been shown through my own experience and in the paper West Coast Main Line the Day Job and Beyond (Green, et al., 2017) to exist in track for a period of 9-18 months before breaking the rail. I theorise from the values of increased loading shown above that it is repeated loading and unloading combined with an inherent weakness, I.E a corrosion pit, that will cause the steel to fail in these scenarios

9.4.10 Conclusions from section 9.4

From the calculations above it is apparent that a reduction in the allowable dip angle significantly reduces the applied load. Taking shear force which is the normal failure mode of rails there is a reduction from 221.304kN at 20mrad to 139.328kN at 10mrad. This is a reduction of 91.976kN.

9.5 Effect of cross sectional area

In this section I propose to look at how the cross sectional area of CEN56 & CEN60 rail profiles affects the structural properties of the rail. CEN60 Rail was introduced in 2000, the profiles are shown in the figures 23 & 24 below. There is no bullhead rail in the passenger lines between Euston and Rugby, so this is excluded from scope. (Network Rail, 2017)

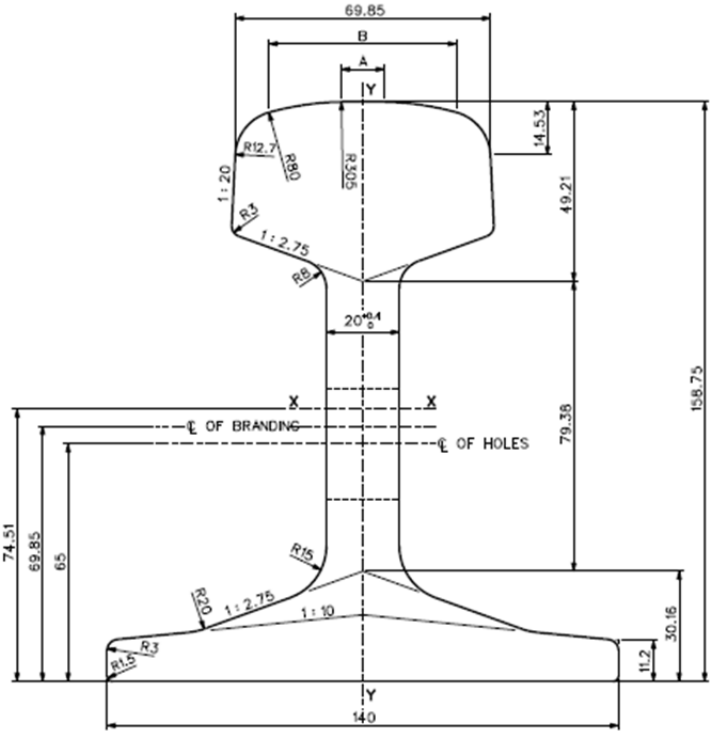

Figure 23 Extract from RE/PW/792 rev A showing the Cross Section of CEN56E1 rail (Ventry, 2005)

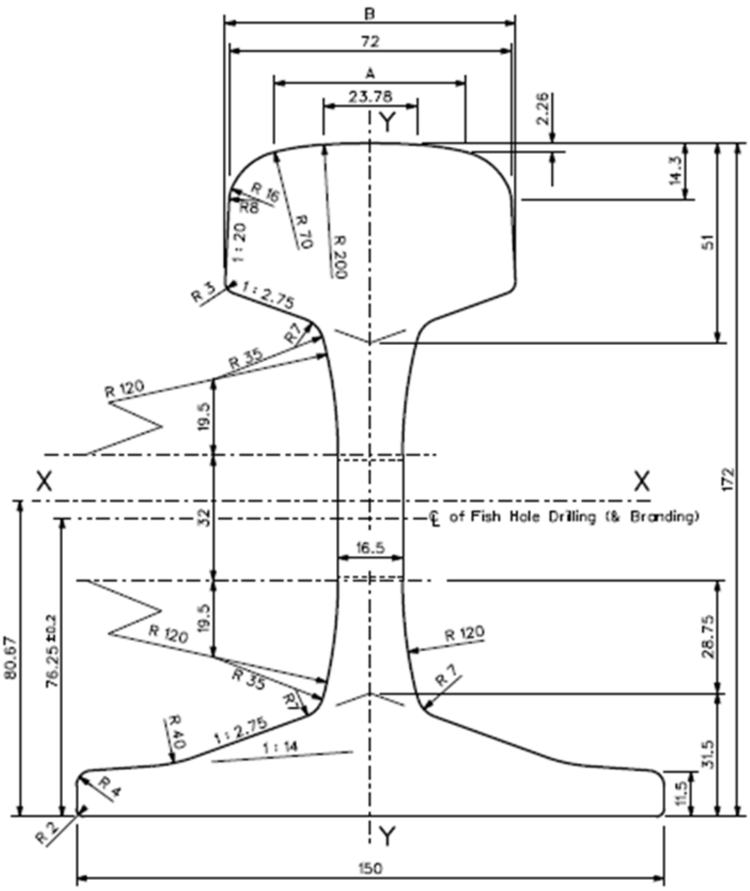

Figure 24 Extract from RE/PW/960 rev A showing the cross section of CEN60E1 rail (Ventry, 2000)

The figures above show the sectional differences between CEN56E1 and CEN60E1 Rail. The Cross sectional areas of these two sections are 7169mm² for CEN56E1 (Ventry, 2005) and 7670mm² for CEN60E1 (Ventry, 2000). This is a seven percent increase in the cross sectional area.

A 7% increase in cross sectional area does not directly convert to a 7% increase in beam strength. The important numbers for the direct comparison of structural beams is the section modulus. The section modulus is a function of area and the theory that most of the work is being done by the extreme fibres of the beam, i.e. the top and the bottom (Build Right, 2017). This holds true with my experience of rail breaks and the details discussed in section 7.1 showing common forms of break emanate from the top of the head or the bottom of the foot of the rail.

Comparing the section modulus of the two rail profiles CEN56E1 has a section modulus of 275.5cm³ at the head of the rail and 311.5cm³ at the foot (Ventry, 2005). CEN60E1 has a section modulus of 333.6cm³ at the head and 375.5cm³ at the foot (Ventry, 2000).

This shows us that the CEN60 profile is twenty one percent stronger at the head. This means the rail would have twenty one percent greater resistance to failures originating in the head i.e. RCF type failures.

The sectional Modulus of CEN60 rail at the foot is also increased by twenty one percent. This means the rail would have twenty one percent greater resistance to failures originating in the foot i.e. tensile failure of the foot.

9.5.1 Change in Cross Sectional Area from Wear

Over long period of time the passage of successive trains wears away fractions of the head of the rail. This is described as headwear. Headwear also occurs through maintenance from grinding or milling of rail. Grinding and milling are required to remove rolling contact fatigue cracking from rails and to maintain optimum rail profile for wheel rail interface. Removal of grinding or milling to reduce headwear is therefore undesirable.

If attrition between the sleeper and the rail is present the foot of the rail can also wear. Loss through this method is described as foot loss.

These two factors together are considered as rail depth, NR/L2/TRK/001 Module 9 (Whitney, et al., 2016) sets out a method for calculating the minimum strength of the rail and using this to determine and to then calculate the minimum allowable depth of the rail.

On the WCML the ultrasonic testing train reports rail depth at an eight weekly interval; this provides data to monitor wear rates and allows sufficient time to change any rails with low depth. Research I have undertaken of historic TEF forms (Network Rail LNW Route, 2016) has shown no instances where rail depth has been cited as a contributory factor to a rail break.

9.5.2 Track Geometry and associated wear types

Curvature changes the way rail wears, sidewear being the most common form of wear in curved rails with headwear becoming a secondary concern. Rolling Contact Fatigue is also a factor more common in curves but can happen in some scenarios on straight track.

The West Coast Main Line is by design a curving route so these factors will both be in appearance on the route.

Sidewear occurs when the vehicle wheels and their flanges interact with the gauge face of the rail. Wear occurs reducing the height of the rail locally on that side (See figure below). On the West Coast Mainline sidewear is measured eight weekly by the Ultrasonic Test Train. Sidewear is measured from 18, unworn, to 0, wear has exceeded allowable limits and a speed restriction must be applied to prevent failure of the rail until re-railing can be completed.

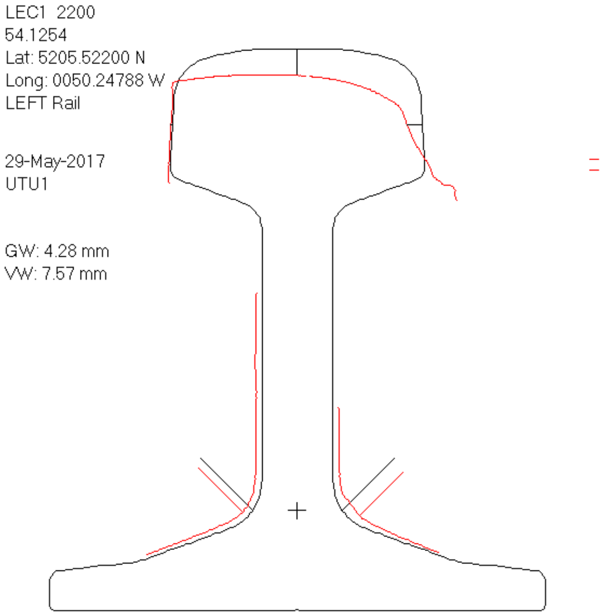

Figure 25 Diagram of sidewear, showing the original rail profile (black) and the worn profile (red) Network Rail Ultrasonic Test Train

Reduction of the profile in this nature reduces the section modulus and strength of the rail. The wear rates are predictable and the frequency of recording means that remedial works can be planned in a suitable length of time to avoid zero sidewear sites.

As discussed, rolling contact fatigue (RCF) and gauge corner cracking can be a cause of a broken rail and with a significant consequence. RCF is caused by creep and eventually plastic flow of the rail metal. This occurs at the area of the contact patch with the train wheel. The contact patch between wheel and rail is approximately the size of a five pence coin. Due to the high loading and relatively small area it is transmitted through, the metal in the area of contact has exceeded its elastic limit and experiences plastic flow. The surrounding material of the rail restrains the small contact patch area however over repeated cycles of loading and unloading high stresses mean that small cracks develop. RCF can be managed by changing the cant and cant deficiency ratios to limit the damage factors, applying suitable lubrication or friction modification or through grinding to remove the cracks before they become significant. However changing track geometry is not always possible due to the interrelationship between the track overhead electrification and structural clearance.

Curves with a cant deficiency greater than 100mm are described as high cant deficiency curves. Wear on these curves will happen in the ways shown above albeit at a more aggressive rate. However they are an important consideration when considering the risk of a broken rail as a derailment whilst the vehicle is undergoing high lateral force would have a more significant consequence.

9.6 Varying support conditions

Track stiffness can be described as the combination of the stiffness of all the components of the track system (defined in section 2.0). Depending on underlying conditions the value of track stiffness can vary significantly. The research paper prepared by the cross industry track stiffness working group (Powrie & Pen, 2016) models a series of stiffness values which have been tested on rail infrastructure. These vary from 80MN/m² (mega newton's per metre squared) to 10MN/m². At 80MN/m² overall track stiffness the rail deflection is less than 1mm at the point of loading, conversely with a system stiffness of 10MN/m² the deflection at rail level is almost 4mm. The rail is thought of as an infinite beam supported on a sprung foundation in these calculations. The stiffness values quoted can be thought of as the spring stiffness.

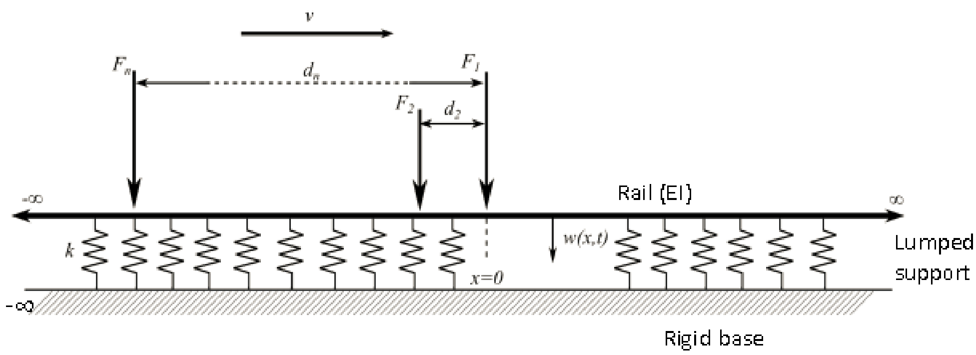

Figure 26 Theoretical beam supported on a sprung foundation (Powrie & Pen, 2016)

Deflections during the loading of the rail will increase the stresses it is withstanding and increase the likelihood of a broken rail so a softer track stiffness is worse from a rail perspective. A higher stiffness also decreases the area over which the load is distributed at ballast, formation and subgrade layers so whilst it is likely to reduce the risk of rail breaks a balance in stiffness will be required to find the optimum whole asset solution in my opinion. This is supported by the article Optimisation of track stiffness on the UK railways (Wehbi & Musgrave, 2017). The article shows that rail stress is decreased with increased stiffness however ballast stresses whilst initially decreasing then starts to increase with increased stiffness.

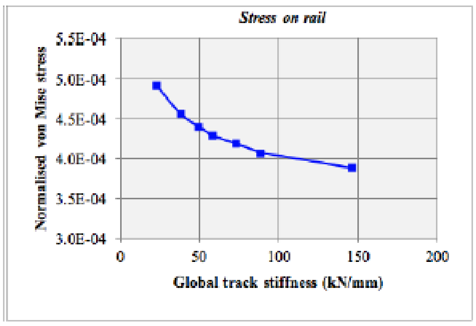

Figure 27 Graphical representation of decreasing rail stress with increased stiffness (Wehbi & Musgrave, 2017)

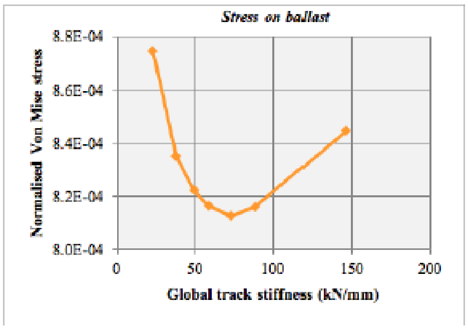

Figure 28 Graphical representation of the relationship between stiffness and ballast stress (Wehbi & Musgrave, 2017)

The variable parts of the system stiffness are as follows:-

The formation and ballast layers, depending on depths and materials used the support will change. Analysis I have carried out using track recording data and ground penetrating radar, sites with soft formation layers are generally the worst performing in terms of deterioration rate of track top. This would also be a contributory factor in rail breaks as insufficient support of the rail from soft formation would lead to deflections and higher internal forces in the rail.

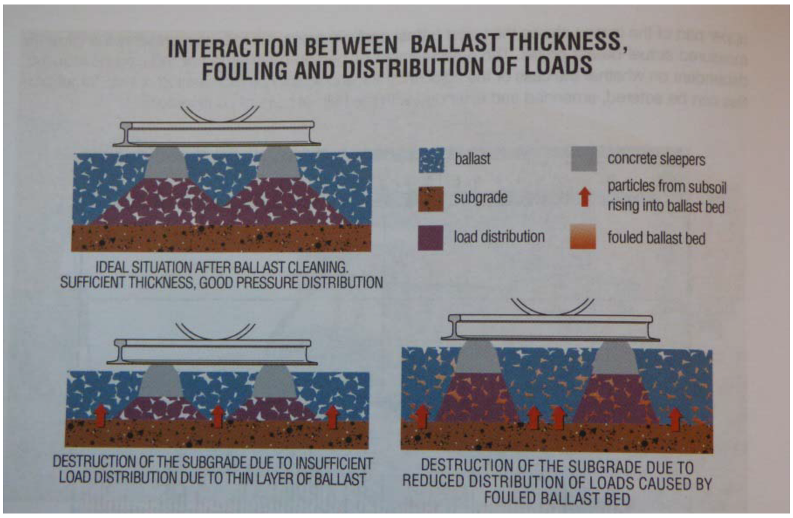

Figure 29 Showing the relative relationship between ballast thickness, fouling and subgrade stresses (Lichtberger, 2005)

The rail seat pad is also variable and serves a primary function of reducing attrition damage between the rail and the concrete sleeper. Removal of this part to increase stiffness would result in damage to both rail and sleeper and is therefore undesirable. Different sleepers have different pads; pre 1990 sleepers are fitted with a 5mm thick pad and post 1990 sleepers a 10mm thick pad. However the deflection and potential to cause additional loading of either style of pad to the rail or the way this is transmitted to the formation and subgrade is minimal when the pads are in optimal condition. 5mm pads however wear out during the life of the sleeper and require replacement prior to the renewal of the sleeper itself. If this has not been done at a suitable time the worn pad can cause damage to the sleeper leading to a dip angle which has been shown in previous sections to increase rail loading, so 5mm pad sleepers which have not been re-padded are an increased risk of broken rails.

Figure 30 Wear to sleeper caused by attrition from worn rail seat pad (Coverdale & Jones, 2011)

Network Rail, LNW Route Business, plans to implement 100% fitment of undersleeper pads on all track renewals from April 2019. As with a rail seat pad this will lower the stiffness of the system overall and so it could be theorised that this will increase the forces in the rail. However research undertaken by Network Rail and Birmingham University (Network Rail, 2015) shows that the inclusion of a stiff undersleeper pad with a track renewal increases the contact area of the sleeper with the ballast by up to 30% (Network Rail, 2015). This increase improves the spread of the load by a similar amount see (figure 24 & 25 below) so a stiff subgrade here would not be subject to the same high point loading as it is with a conventional sleeper. This has an additional benefit of reducing deterioration of top by up to 60% (Network Rail, 2015) meaning the track system will stay stiffer for longer between maintenance interventions this will reduce forces experienced in the rail and reduce the risk of a broken rail by increasing the overall stiffness of the system over its whole life.

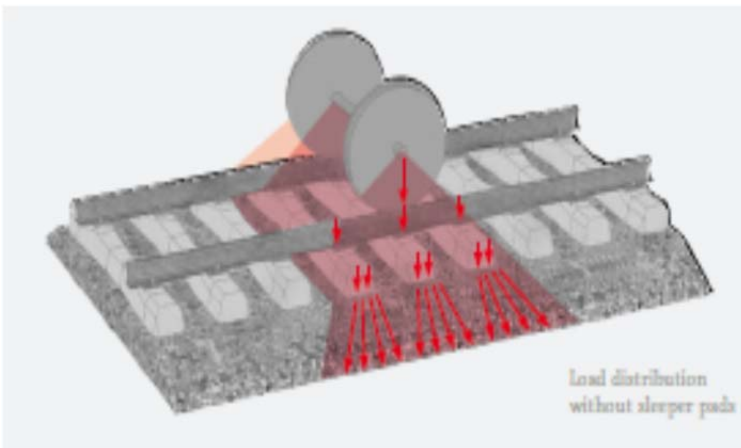

Figure 31 Load distribution to subgrade form a conventional concrete sleeper (Network Rail, 2015)

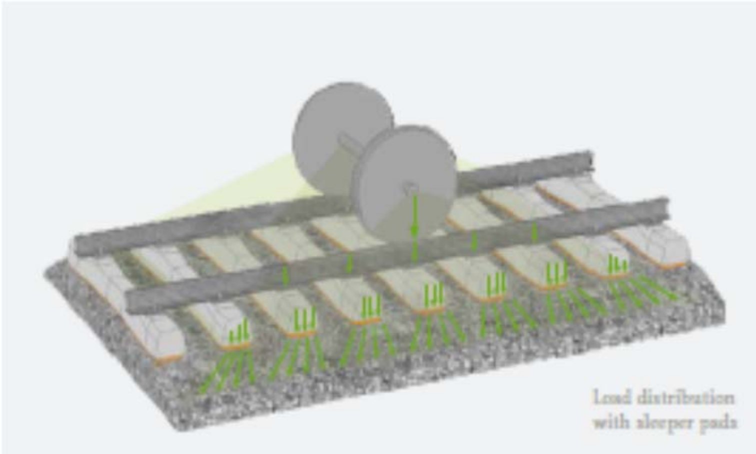

Figure 32 Load distribution to the subgrade from concrete sleepers with Undersleeper pads (Network Rail, 2015)

A further consideration is a short area of significantly stiffer track stiffness. Likely causes of this are either a structure under the railway with a reduced ballast depth and insufficient transition arrangements back to the standard ballasted formation, or a localised formation failure which has created a wet-bed which has then become solid through drying out. A hard point like this would increase the loading in two ways. Firstly as shown in ‘ A guide to track bed stiffness’ (Powrie & Pen, 2016) deflections in the transition off the structure can be as high as 9mm reducing down to less than 1mm at the structure itself over a distance of less than 2m.

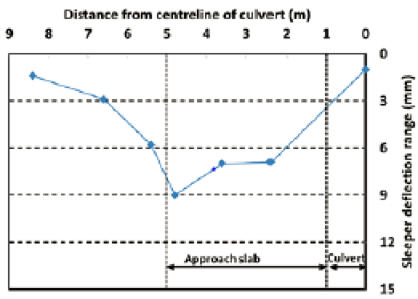

Figure 33 Deflections vertically on the approach to a reduced ballast depth structure (Powrie & Pen, 2016)

This has a twin impact on the forces within the rail firstly as discussed in the previous paragraphs large deflections in the rail increase the strain being exerted and the bending moment. Secondly a transition over such a short distance from poorly supported track to very stiff track will excite the vehicle creating an impact loading at the structure itself. A significant wetbed is also likely to respond in a similar manner due to soft surrounding track stiffness from formation failure and the wetbed itself setting hard in the summer dry period.

[redacted]

Figure 34 Example Wetbed

A further way which deflection may occur in the rail is ‘voiding’ or ‘hanging’ of the track the effects of this would be as other kinds of deflection discussed earlier in this section of the report.

9.7 Changes to sleeper spacing’s

Given the findings of previous sections, firm support of the rail is shown as key to lowering the stresses in the rail. On high cant deficiency curves sleeper spacing is closed to 600mm centres (Whitney, et al., 2016). In this section I will re-calculate the shear stress in the beam AB for the Class 390 dynamic loading to ascertain if this is improved.

9.7.1 Shear stress in Beam AB with length of 600mm

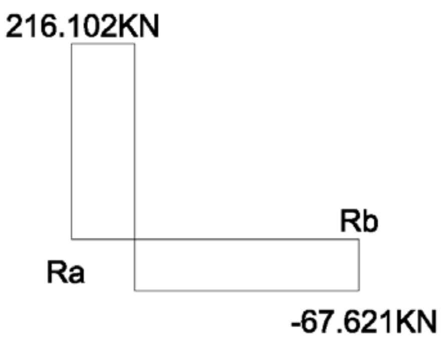

Figure 35 Shear stress for 600mm sleeper spacing

As can been seen in the figure above and the supporting calculations in Appendix A the reduction in maximum shear force is 5.202KN relative to the forces in question this reduction can be considered negligible.

9.8 Rail Defects due to Damage

Figure 36 Damaged rail due to excavator impact (Image courtesy of Robert Langford)

Damage can occur to rails due to external influences, most commonly, the incorrect use of on track machines. The effect of this would be to reduce the section modulus and thus strength of the rail. Due to the unpredictable nature of this failure mode I have disregarded it for the final model.

9.9 Hostile Operating Environment (Corrosion)

The paper 'West Coast Main Line The Day Job and Beyond' (Green, et al., 2017) discussed at length the reduced service life of rails in Kilsby Tunnel due to hostile operating environment. Two broken rails occurred in the tunnel in 2016. The root cause of the two breaks was tensile foot failure, the rate at which the failure had manifested had been accelerated by water entering the tunnel through the structure lining as shown in figures 37 & 38. I visited the site in June 2017 jointly with other disciplines. It was clear that water entering the structure was not being properly managed and that corrosion from the water was the root cause of the breaks. The best solution would be better management of the drainage here. However in the interim the risk of a rail break at the locations with drainage problems is higher and any risk model should consider this.

Figure 37 Example ineffective structure drain Kilsby Tunnel

Figure 38 Example standing water causing track deterioration Kilsby Tunnel

10.0 Conclusions

In conclusion to this report I have gathered sufficient data to produce a draft version of a broken rail modelling tool. I consider the highest risk areas to be as follows:-

- 125mph running areas due to high dynamic loading.
- Dip angles particularly where these have been present for extended periods due to a fatigue effects from impact loadings

- Changes of dynamic track stiffness including formation problems such as wetbeds and structures with reduced ballast depth.

I have collated all the findings of this report and created the ‘WCML Broken Rail Risk Tool’. Outputs from the tool can be found in Appendix B.

11.0 Future development

I intend to present the final draft tool to LNW Route Business for consideration with the suggestion of using it to evaluate data from the New Measurement Train Trace. The parameters I have set for the various risk factors are, I feel, in line with the analysis of loading in this report. A period of testing will be needed to check that these hold true with actual observations from the railway under traffic. The tool can be developed with further rolling stock for use on other routes away from the West Coast Main Line if it proves a success in a trial period.

[redacted]

12.0 References

4rail.net, 2004-2010. *4rail.net - High Speed Trains - Pendolino.* [Online]
Available at: http://www.4rail.net/ref_fast_pendolino.php
[Accessed 15 June 2017].

Boocock, D. & Mitchell, J. R., 1995. *GMRC2513 Commentary on Permissible Track Forces for Railway Vehicles.* s.l.:British Railways Board.

British Railways Board, 1993. *GM/TT0088 Permissible Track Forces for Railway Vehicles Issue 1 Revision A,* London: Railway Group Standards.

Build Right, 2017. *Sectional Properties.* [Online]
Available at:
https://www.dlsweb.rmit.edu.au/toolbox/buildright/content/bcgbc4010a/03_properties/02_section_properties/page_007.htm
[Accessed 16 August 2017].

Coverdale, S. & Jones, A., 2011. *CP5 Track Asset Policy.* s.l.:Network Rail.

Downes, M., Edgley, J. & McManus, M., 2016. *NR/L3/TRK/2049 Network Rail Track Design Handbook Issue 13.* s.l.:Network Rail.

Evans, E., Jones, A. & McManus, M., 2009. *NR/L2/TRK/8100 Railway Ballast and Stoneblower Aggregate Issue 4.* s.l.:s.n.

Green, C., Fasham, R. & Quigley, R., 2017. *West Coast Main Line The Day Job and Beyond.* Birmingham: The Permanent Way Institution.

Lichtberger, B., 2005. *Track Compendium: Formation, Permanent Way, Maintenance, Economics.* s.l.:s.n.

Network Rail LNW Route, 2016. *TEF3064 - Hazard Report for Track Assets,* s.l.: Network Rail.

Network Rail, 2015. *Undersleeper Pads Head of Track Presentation,* London: Network Rail.

Network Rail, 2017. *GEOGIS DATABASE,* London: Network Rail.

Network Rail, 2017. *Route Availability Webpage.* [Online]
Available at: http://archive.nr.co.uk/aspx/10551.aspx
[Accessed 12 March 2017].

NR/GN/TRK/7001/TWI3T046/Video9 Track Recording Vehicle Vertical Level or Top Fault. 2013. [Film] Directed by Network Rail. s.l.: s.n.

Office of Rail Regulation, 2006. *Train Derailment at Hatfield: A Final Report by the Independant Investigation Board,* s.l.: Office of Rail Regulation.

Powrie, W. & Pen, L. L., 2016. *A Guide To Track Stiffness.* s.l.:University of Southampton.

RAIB, 2017. *Class investigation into rail breaks on East Coast Main Line,* s.l.: ORR.

RSSB, 2015. *GO/RT3056 Principals of safe freight train operation.* s.l.:RSSB - Railway Group Standards.

The Permanent Way Institution, 2014. *Understanding Track Engineering.* s.l.:The Permanent Way Institution.

Ventry, D., 2000. *CEN60E1 (UIC60) Rail Section, Drilling Details and Bond Hole Limits RE/PW/901.* s.l.:Network Rail.

Ventry, D., 2005. *CEN56E1 Rail Section and Drilling Details RE/PW/792.* s.l.:Network Rail.

Ventry, D., Morris, G. & McNaughton, A., 2002. *RT/CE/S/012 Cast Austenitic Manganese Steel Crossings Issue 2.* s.l.:Railtrack.

Webb, D., 2013. *Letter of Instruction 15722.* s.l.:Network Rail.

Wehbi, M. & Musgrave, P., 2017. Optimisation of track stiffness on the UK railways. *The Journal Volume 135 Part 3 Permanent Way Institution,* pp. 24-31.

Whitney, B., 2015. *Rail Breaks / Track Stiffness,* Milton Keynes: Network Rail .

Whitney, B., Edgley, J. & McManus, M., 2016. *NR/L2/TRK/2102 Design and Construction of Track Issue 8.* London(Greater London): Network Rail.

Whitney, B., Evans, G. & McManus, M., 2017. *NR/L2/TRK/001 Inspection and Maintenance of Permanent Way Issue 11.* s.l.:Network Rail.

Appendix A – Supporting Calculations

Calculations are referenced to the section of the document that they relate.

Supporting Calculations 9.1.1

$$\sum VF = 0$$

$$\sum VF = Ra + Rb - 124.544$$

$$Ra + Rb = 124.544$$

I can now take moments about Ra to solve for Rb and then Ra.

$$\sum MA = 0$$

$$\sum MA = 124.544(0.325) - Rb(0.65)$$

$$Rb = 124.544(0.325) \div 0.65$$

$$Rb = 62.272KN$$

Ra=124.544-62.272

$$Ra = 62.272\text{KN}$$

Supporting Calculations 9.1.3

$$\sum MC = 0$$

$$0 = MC + 124.544(0) - 62.272(0.325)$$

$$MC = 62.272(0.325) - 124.544(0)$$

$$MC = 20.238KNM$$

Supporting Calculations 9.1.7

$$\sum VF = 0$$

$$\sum VF = Ra + Rb - 124.544$$

$$Ra + Rb = 124.544$$

I can now take moments about Ra to solve for Rb and then Ra.

$$\sum MA = 0$$

$$\sum MA = 124.544(0.143) - Rb(0.65)$$

$$Rb = 124.544(0.143) \div 0.65$$

$$Rb = 27.400KN$$

Ra=124.544-27.4

$$Ra = 97.144\text{KN}$$

Supporting Calculations 9.1.9

$$\sum MC = 0$$

$$0 = MC + 124.544(0) - 97.144(0.143)$$

$$MC = 97.144(0.143) - 124.544(0)$$

$$MC = 13.891KNM$$

Supporting Calculations 9.2.1

I will be using the following formula taken from the group standard

$$P2 = Q + (Az\ x\ Vm\ x\ M\ x\ C\ x\ K)$$

First I will calculate M

$$M = (\frac{Mv}{Mv + Mz})^{0.5}$$

$$M = (\frac{1000}{1000 + 245})^{0.5}$$

$$M = 0.896$$

Then I will Calculate C

$$C = 1 - \left(\frac{\pi\ x\ Cz}{4[Kz(Mv + Mz)]^{0.5}}\right)$$

$$C = 1 - \left(\frac{\pi\ x\ 55.4x10^{3}}{4[62.0x10^{6}(1000 + 245)]^{0.5}}\right)$$

$$C = 1 - \left(\frac{174044.233}{4[7.719x10^{10}]^{0.5}}\right)$$

$$C = 1 - (\frac{174044.233}{1111323.535})$$

$$C = 0.843$$

Finally I will calculate K

$$K = (Kz\ x\ Mv)^{0.5}$$

$$K = (62.0x10^{6}\ x1000)^{0.5}$$

$$K = 248997.992$$

I can now substitute in for P2

$$P2 = Q + (Az\ x\ Vm\ x\ M\ x\ C\ x\ K)$$

$$P2 = 73549.875 + (0.020\ x\ 55.88\ x\ 0.896\ x0.843\ x\ 248997.992)$$

$$P2 = 73549.875 + 210192.794$$

$$P2 = 283742.669N$$

Supporting Calculations 9.2.2

Again I will be using the following formula from the Group Standard.

$$P2 = Q + (Az\ x\ Vm\ x\ M\ x\ C\ x\ K)$$

First I will calculate M

$$M = (\frac{Mv}{Mv + Mz})^{0.5}$$

$$M = (\frac{950}{950 + 245})^{0.5}$$

$$M = 0.892$$

Then I will Calculate C

$$C = 1 - \left(\frac{\pi \, x \, Cz}{4[Kz(Mv + Mz)]^{0.5}}\right)$$

$$C = 1 - \left(\frac{\pi \, x \, 55.4x10^{3}}{4[62.0x10^{6}(950 + 245)]^{0.5}}\right)$$

$$C = 1 - \left(\frac{174044.233}{4[7.409x10^{10}]^{0.5}}\right)$$

$$C = 1 - (\frac{174044.233}{1088779.133})$$

$$C = 0.840$$

Finally I will calculate K

$$K = (Kz \, x \, Mv)^{0.5}$$

$$K = (62.0x10^{6} \, x950)^{0.5}$$

$$K = 242693.222$$

I can now substitute in for P2

$$P2 = Q + (Az \, x \, Vm \, x \, M \, x \, C \, x \, K)$$

$$P2 = 124544 + (0.020 \, x \, 33.53 \, x \, 0.892 \, x0.840 \, x \, 242693.222)$$

$$P2 = 124544 + 121945.376$$

$$P2 = 246489.376N$$

Supporting Calculations 9.3.1

$$P2 = Q + (Az \, x \, Vm \, x \, M \, x \, C \, x \, K)$$

$$P2 = 73549.875 + (\mathbf{0.030} \, x \, 55.88 \, x \, 0.896 \, x0.843 \, x \, 248997.992)$$

$$P2 = 73529.875 + 315289.190$$

$$P2 = 388819.065N$$

Supporting Calculations 9.3.3

$$P2 = Q + (Az \, x \, Vm \, x \, M \, x \, C \, x \, K)$$

$$P2 = 73549.875 + (\mathbf{0.010}\ x\ 55.88\ x\ 0.896\ x 0.843\ x\ 248997.992)$$

$$P2 = 73529.875 + 105096.397$$

$$P2 = 178626.272N$$

Supporting Calculations 9.3.4

$$P2 = Q + (Az\ x\ Vm\ x\ M\ x\ C\ x\ K)$$

$$P2 = 73549.875 + (\mathbf{0.004}\ x\ 55.88\ x\ 0.896\ x 0.843\ x\ 248997.992)$$

$$P2 = 73529.875 + 42038.559$$

$$P2 = 115588.434N$$

Supporting Calculations 9.4.3

$$\sum VF = 0$$

$$\sum VF = Ra + Rb - 283.723$$

$$Ra + Rb = 283.723$$

I can now take moments about Ra to solve for Rb and then Ra.

$$\sum MA = 0$$

$$\sum MA(0.143) - Rb(0.65)$$

$$Rb = 283.723(0.143) \div 0.65$$

$$Rb = 62.419KN$$

Ra=283.723-62.419

$$Ra = 221.304\text{KN}$$

Supporting Calculations 9.4.5

$$\sum MC = 0$$

$$0 = MC + 283.723(0) - 221.304(0.143)$$

$$MC = 221.304(0.143) - 283.723(0)$$

$$MC = 31.646KNM$$

Supporting Calculations 9.7.1

$$\sum VF = 0$$

$$\sum VF = Ra + Rb - 283.723$$

$$Ra + Rb = 283.723$$

I can now take moments about Ra to solve for Rb and then Ra.

$$\sum MA = 0$$

$$\sum MA(0.143) - Rb(0.600)$$

$$Rb = 283.723(0.143) \div 0.600$$

$$Rb = 67.621KN$$

Ra=283.723-67.621

$$Ra = 216.102\text{KN}$$

$$\sum MC = 0$$

$$0 = MC + 283.723(0) - 216.102(0.143)$$

$$MC = 216.102(0.143) - 283.723(0)$$

$$MC = 30.902KNM$$

Appendix B - Sample WCML Broken Rail Risk Tool Outputs

WCML Broken Rail Risk Tool

Dynamic Load calculator - Group Standard GM/TT0088 Issue1

Select vehicle	Fully Laden Freight	Static Wheel Load (N)	124544.000		
Enter Permissable Speed (Mph)	125	Vehicle's Max Speed	75	Max speed (m/s)	33.528
Mv Value, Unsprung mass (Kg)	950				
Enter Dip Angle Value (Mrad)	30	Az Value	0.030		
M Value	0.892	C Value	0.840	K Value	242693.222

P2 - Site Dynamic Load (KN)	307.404

Additional Risk Factors

Dynamic loading risk factor		10
Dip Angle time in track?	Less than 6 months	12
Rail Age?	15 Years or Less	12
Rail Grade?	CEN60	10
Sidewear of 5 or less?	Yes	12
Minimum rail depth?	Yes	14
Rail Seat Pad?	10mm	14
Formation issues?	No	14
Underbridge or Culvert?	Yes	17
High corrosion?	No	17

Final Risk Rating	LOW RISK

WCML Broken Rail Risk Tool created by Richard Quigley for Network Rail 23/08/2017

Please contact *richard.quigley@networkrail.co.uk* for further information or amendments

WCML Broken Rail Risk Tool

Dynamic Load calculator - Group Standard GM/TT0088 Issue1

Select vehicle	Super Voyager Class 22	Static Wheel Load (N)	69872.381		
Enter Permissable Speed (Mph)	125	Vehicle's Max Speed	125	Max speed (m/s)	55.88
Mv Value, Unsprung mass (Kg)	1000				
Enter Dip Angle Value (Mrad)	11	Az Value	0.011		
M Value	0.896	C Value	0.843	K Value	248997.992

P2 - Site Dynamic Load (KN)	185.561

Additional Risk Factors

Dynamic loading risk factor		5
Dip Angle time in track?	Less than 6 months	6
Rail Age?	25 Years or Less	9
Rail Grade?	CEN56 (BS113A)	9
Sidewear of 5 or less?	No	9
Minimum rail depth?	No	9
Rail Seat Pad?	5mm	14
Formation issues?	Drainage problems	15
Underbridge or Culvert?	Yes	18
High corrosion?	Wet Tunnel	27

Final Risk Rating	MEDIUM RISK

WCML Broken Rail Risk Tool created by Richard Quigley for Network Rail 23/08/2017

Please contact *richard.quigley@networkrail.co.uk* for further information or amendments

WCML Broken Rail Risk Tool

Dynamic Load calculator - Group Standard GM/TT0088 Issue1

Select vehicle	Pendolino Class 390	Static Wheel Load (N)	73549.875		
Enter Permissable Speed (Mph)	125	Vehicle's Max Speed	125	Max speed (m/s)	55.88
Mv Value, Unsprung mass (Kg)	1000				
Enter Dip Angle Value (Mrad)	30	Az Value	0.030		
M Value	0.896	C Value	0.843	K Value	248997.992
P2 - Site Dynamic Load (KN)		389.063			

Additional Risk Factors

Dynamic loading risk factor		10
Dip Angle time in track?	Greater than 6 Months	80
Rail Age?	25 Years or Less	120
Rail Grade?	CEN56 (BS113A)	120
Sidewear of 5 or less?	No	120
Minimum rail depth?	No	120
Rail Seat Pad?	5mm	180
Formation issues?	Drainage problems	198
Underbridge or Culvert?	No	198
High corrosion?	No	198
Final Risk Rating	HIGH RISK	

WCML Broken Rail Risk Tool created by Richard Quigley for Network Rail 23/08/2017

Please contact *richard.quigley@networkrail.co.uk* for further information or amendments